Journal of Solid Mechanics Vol. 10, No. 2 (2018) pp. 450-463

Elastic-Plastic Transition of Pressurized Functionally Graded Orthotropic Cylinder using Seth's Transition Theory

S. Sharma *, R. Panchal

Department of Mathematics, Jaypee Institute of Information Technology, Noida, India

Received 28 March 2018; accepted 25 May 2018

ABSTRACT

In this paper the radial deformation and the corresponding stresses in a functionally graded orthotropic hollow cylinder with the variation in thickness and density according to power law and rotating about its axis under pressure is investigated by using Seth's transition theory. The material of the cylinder is assumed to be non-homogeneous and orthotropic. This theory helps to achieve better agreement between experimental and theoretical results. Results has been mentioned analytically and numerically. From the analysis, it has been concluded that cylinder made up of orthotropic material whose thickness increases radially and density decreases radially is on the safer side of the design as circumferential stresses are high for cylinder made up of isotropic material as compared to orthotropic material. This paper is based on elastic-plastic behavior which plays important role in practical design of structures for safety factor.

Keywords: Elastic-plastic; Orthotropic; Pressure; Functionally graded material; Cylinder.

1 INTRODUCTION

ORTHOTROPIC structures are very common in present day engineering. Orthotropic cylinder has gained widespread use and acceptance, and has already earned worldwide popularity in almost all kinds of applications, housing, marine, highway bridge deck, aerospace and for strengthening of structures. In recent years, the problem of elastic-plastic deformation in composite cylinders made up of functionally graded materials (FGMs) operating at high pressure and temperature has attracted the interest of the many researchers. For an improved usage of the material, it is necessary to allow variation of the effective material properties in one direction of cylinders. The analysis of rotating functionally graded orthotropic cylinders has been reported rarely in the literature. Author A.F. Bower [1] has mentioned the behavior of orthotropic cylinders and E.J. Hearn [2] discussed the anisotropic behavior of materials. G.H. Kim et al. [3] investigated the several fracture problems using new interaction integral formulation and compared the result with analytic solutions. A.M. Zenkour [4] determined the analytic solutions for the rotating orthotropic cylinders of variable and uniform thickness and concluded that varying thickness in cylinders shows excellent result. S. Dag [5] gave a new computational technique based on the equivalent domain integral (EDI) for fracture analysis of orthotropic functionally graded materials subjected to thermal stresses and

*Corresponding author.
E-mail address: sanjiit12@rediffmail.com (S.Sharma)

concluded that among the three principal thermal expansion coefficient components, the in-plane component perpendicular to the crack axis has the foremost vital influence on the stress intensity factor. M. Paschero et al. [6] analyzed the buckling of an axially-loaded orthotropic circular cylinder by defining orthotropic material properties in terms of associated geometric mean. H.M. Wang [7] has obtained closed form solutions for pressurized orthotropic cylinders using the Lame's equations and result obtained shows good agreement with numerical simulation results using finite element analysis. G.J. Nie et al. [8] determined analytically static plane-strain deformations of functionally graded orthotropic cylinders with elliptic inner and circular outer surfaces. Authors solved the problem by employing Fourier and the Frobenius series using the assumption that four relevant elastic moduli are with same variation in the radial direction. S. Sharma et al. [9] determined thermal creep stresses and strain rates in a functionally graded stainless steel composite cylinder using finite difference method and concluded that material anisotropy may have beneficial effect on stresses. The result obtained using small strain theory is found to be on unsafe side when compared to those obtained using finite strain theory. Seth's transition theory act as a bench mark in dealing with the problems of elastic-plastic and creep deformation i.e. applied by various authors i.e. S.K. Gupta et al. [10] determined the stresses for orthotropic rotating cylinder. B.N Borah [11] investigated the stresses in tubes and mentioned the transition points. A.K. Aggarwal et.al. [12] concluded that by introducing a suitably chosen temperature gradient, non-homogeneous compressible circular cylinder with internal and external pressure for non-linear measure is on the safer aspect of the design as compared to the cylinder without temperature. S. Sharma et al. [13] investigated stresses in transversely isotropic cylinder under pressure and concluded that transversely isotropic cylinder is on safer side as compared to isotropic cylinder. Safety analysis has been done for the torsion of a functionally graded thick-walled circular cylinder under internal and external pressure subjected to thermal loading by S. Sharma et al. [14] and concluded that in creep torsion cylinder made up of less functionally graded material under pressure is better choice for designing point of view as compared to homogeneous cylinder.

2 OBJECTIVE OF THE STUDY

In order to clarify the transition from elastic to plastic state, firstly, we need to recognize transition state as an asymptotic one and in this present study, it is our main aim to eliminate the necessity of yield condition, elastic-plastic, jump conditions and semi-empirical laws etc. The objective of this paper is to calculate stresses for thick-walled functionally graded rotating orthotropic cylinder under internal and external pressure using the concept of transition theory which will act as a benchmark and helpful in practical design of orthotropic cylinder.

3 MATHEMATICAL FORMULATION

Consider a thick-walled orthotropic cylinder made up of functionally graded material with internal and external radii a and b respectively, subjected to internal and external pressure p_1 and p_2 respectively. The non-homogeneity in the cylinder is due to variation of thickness, density and compressibility C. In cylindrical polar co-ordinates, the components of displacements are given as:

$$u = r(1-\kappa),\ v = 0 \text{ and } w = dz, \tag{1}$$

where κ is a function of r only and d is a constant.

Seth has defined the generalized principal strain measure e_{ii} by taking the integral of the weighted function as:

$$e_{ii} = \int_0^{e_{ii}^A} [1-2e_{ii}^A]^{\frac{n}{2}-1} de_{ii}^A = \frac{1}{n}\left[1-(1-2e_{ii}^A)^{\frac{n}{2}}\right] \quad (i = 1,2,3), \tag{2a}$$

where n is the measure and e_{ii}^A are the principal finite components of strain.

Using (2a) the generalized components of strain are,

$$e_{rr} = \frac{1}{n}\left[1-(r\kappa'+\kappa)^{n}\right], e_{\theta\theta} = \frac{1}{n}\left[1-\kappa^{n}\right], e_{zz} = \frac{1}{n}[1-(1-d)^{n}], e_{r\theta} = e_{\theta z} = e_{zr} = 0, \tag{2b}$$

where n is the non-linear measure and $\kappa' = \dfrac{d\kappa}{dr}$.

The component of stress for orthotropic material is given as:

$$\begin{aligned}
&\tau_{rr} = \frac{C_{11}}{n}[1-(r\kappa'+\kappa)^{n}] + \frac{C_{12}}{n}[1-\kappa^{n}] + \frac{C_{13}}{n}[1-(1-d)^{n}], \tau_{\theta\theta} = \frac{C_{21}}{n}[1-(r\kappa'+\kappa)^{n}] + \frac{C_{22}}{n}[1-\kappa^{n}] + \frac{C_{23}}{n}[1-(1-d)^{n}],\\
&\tau_{zz} = \frac{C_{31}}{n}[1-(r\kappa'+\kappa)^{n}] + \frac{C_{32}}{n}[1-\kappa^{n}] + \frac{C_{33}}{n}[1-(1-d)^{n}],
\end{aligned} \tag{3}$$

where $\tau_{rr}, \tau_{\theta\theta}$ and τ_{zz} are the radial, circumferential and axial stresses respectively.

Taking non-homogeneity in orthotropic material [7] as:

$$\begin{aligned}
&C_{11} = C_{011}\left(\frac{r}{b}\right)^{-k}, C_{12} = C_{012}\left(\frac{r}{b}\right)^{-k}, C_{13} = C_{013}\left(\frac{r}{b}\right)^{-k}, C_{21} = C_{021}\left(\frac{r}{b}\right)^{-k}, C_{22} = C_{022}\left(\frac{r}{b}\right)^{-k},\\
&C_{23} = C_{023}\left(\frac{r}{b}\right)^{-k}, C_{31} = C_{031}\left(\frac{r}{b}\right)^{-k}, C_{32} = C_{032}\left(\frac{r}{b}\right)^{-k}, C_{33} = C_{033}\left(\frac{r}{b}\right)^{-k},
\end{aligned} \tag{4}$$

where $a \le r \le b, k(\le 0)$ is non-homogeneity parameter and $C_{011}, C_{012}, C_{013}, C_{021}, C_{022}, C_{023}, C_{031}, C_{032}, C_{033}$ are material constants.

Using Eq. (4) in Eq. (3) we get,

$$\begin{aligned}
\tau_{rr} &= \frac{C_{011}(\frac{r}{b})^{-k}}{n}[1-(r\kappa'+\kappa)^{n}] + \frac{C_{012}(\frac{r}{b})^{-k}}{n}[1-\kappa^{n}] + \frac{C_{013}(\frac{r}{b})^{-k}}{n}[1-(1-d)^{n}],\\
\tau_{\theta\theta} &= \frac{C_{021}(\frac{r}{b})^{-k}}{n}[1-(r\kappa'+\kappa)^{n}] + \frac{C_{022}(\frac{r}{b})^{-k}}{n}[1-\kappa^{n}] + \frac{C_{023}(\frac{r}{b})^{-k}}{n}[1-(1-d)^{n}],\\
\tau_{zz} &= \frac{C_{031}(\frac{r}{b})^{-k}}{n}[1-(r\kappa'+\kappa)^{n}] + \frac{C_{032}(\frac{r}{b})^{-k}}{n}[1-\kappa^{n}] + \frac{C_{033}(\frac{r}{b})^{-k}}{n}[1-(1-d)^{n}],
\end{aligned} \tag{5}$$

$\tau_{r\theta} = \tau_{\theta z} = \tau_{zr} = 0$, where τ_{ij}, e_{ij} are stress and strain tensors respectively.

Equations of equilibrium [10] is given as,

$$\frac{d}{dr}\left(hr\tau_{rr}\right) - h\tau_{\theta\theta} + h\rho\omega^{2}r^{2} = 0, \tag{6}$$

where $h = h_0\left(\frac{r}{b}\right)^{-t}$ is the wall thickness of the rotating cylinder, $\rho = \rho_0\left(\frac{r}{b}\right)^{-q}$ is the density of the rotating cylinder, ω is the angular speed of the rotating cylinder.

4 IDENTIFICATION OF TRANSITION POINT

When a deformable solid is subjected to internal and external loading, it has been observed that the solid first deforms elastically. If the loading is sustained, plastic flow might set in. So, there exists an intermediate state in between elastic and plastic state that is known as transition state. Thus, differential system defining the elastic state should reach a critical value in the transition state. The nonlinear differential equation at transition state is obtained by substituting, Eq. (5) in Eq. (6), as:

$$\frac{d\kappa}{dP}[hP(P+1)^n+\frac{C_{012}(\frac{r}{b})^{-k}}{C_{011}(\frac{r}{b})^{-k}}hP-\frac{\rho\omega^2r^2h}{nC_{011}(\frac{r}{b})^{-k}\kappa^n}+\frac{h}{nC_{011}(\frac{r}{b})^{-k}\kappa^n}[\{(k+t-1)C_{011}(\frac{r}{b})^{-k}+C_{021}(\frac{r}{b})^{-k}\}\{1-\kappa^n(P+1)^n\}$$
$$+\{(k+t-1)C_{012}(\frac{r}{b})^{-k}+C_{022}(\frac{r}{b})^{-k}\}\{1-\kappa^n\}+\{(k+t-1)C_{013}(\frac{r}{b})^{-k}+C_{023}(\frac{r}{b})^{-k}\}\{1-(1-d)^n\}]+h\kappa P(P+1)^{n-1}=0, \quad (7)$$

where $r\kappa' = P\kappa$.

The transition points of k in Eq. (5) are $P\to 0, P\to -1$ and $P\to\pm\infty$.

The boundary conditions are

$$\tau_{rr}=-p_1 \text{ at } r=a \text{ and } \tau_{rr}=-p_2 \text{ at } r=b. \quad (8)$$

The resultant force normal to plane Z = constant must vanish, i.e.

$$\int_a^b r\tau_{zz}dr=0. \quad (9)$$

5 TRANSITIONAL AND PLASTIC STRESSES

As elastic state can go to plastic state under internal and external loading through a transition state, thus it has been shown [10-13] that the asymptotic solution through principal stress leads from elastic state to plastic state at transition point $P\to\pm\infty$. To determine the plastic stresses at the transition point $P\to\pm\infty$, we define the transition function TR in terms of τ_{rr} as:

$$TR=1-\frac{n\tau_{rr}}{C_{011}\left(\frac{r}{b}\right)^{-k}+C_{012}\left(\frac{r}{b}\right)^{-k}+C_{013}\left(\frac{r}{b}\right)^{-k}}-\frac{n\rho\omega^2r^2}{2(C_{011}\left(\frac{r}{b}\right)^{-k}+C_{012}\left(\frac{r}{b}\right)^{-k}+C_{013}\left(\frac{r}{b}\right)^{-k})}. \quad (10)$$

Using the value of τ_{rr} from Eq. (3) in Eq. (10)

$$TR=\frac{1}{C_{011}\left(\frac{r}{b}\right)^{-k}+C_{012}\left(\frac{r}{b}\right)^{-k}+C_{013}\left(\frac{r}{b}\right)^{-k}}[C_{011}\left(\frac{r}{b}\right)^{-k}\kappa^n(P+1)^n+C_{012}\left(\frac{r}{b}\right)^{-k}\kappa^n+C_{013}\left(\frac{r}{b}\right)^{-k}(1-d)^n-\frac{n\rho\omega^2r^2}{2}]. \quad (11)$$

Taking the logarithmic differentiation of Eq. (11), one gets

$$\frac{d\log TR}{dr}=\frac{k}{r}+\frac{n\beta^nC_{011}(\frac{r}{b})^{-k}}{rR(C_{011}+C_{012}+C_{013})(\frac{r}{b})^{-k}}[P(P+1)^{n-1}\kappa\frac{dP}{d\kappa}+(P+1)^n+\frac{C_{012}(\frac{r}{b})^{-k}}{C_{011}(\frac{r}{b})^{-k}}P-\frac{k}{n}\{(P+1)^n+\frac{C_{012}(\frac{r}{b})^{-k}}{C_{011}(\frac{r}{b})^{-k}}$$
$$+\frac{C_{013}(\frac{r}{b})^{-k}}{C_{011}(\frac{r}{b})^{-k}\kappa^n}(1-d^n)\}-\frac{\rho\omega^2r^2(2-q)}{2C_{011}(\frac{r}{b})^{-k}\kappa^n}]. \quad (12)$$

Substituting the value of $\dfrac{dP}{d\kappa}$ in Eq. (12) from Eq. (7), we get

$$\frac{d\log TR}{dr}=\frac{k}{r}+\frac{n\kappa^n C_{011}(\frac{r}{b})^{-k}}{rR(C_{011}+C_{012}+C_{013})(\frac{r}{b})^{-k}}[\frac{-1}{h}\{hP(P+1)^n+\frac{C_{012}(\frac{r}{b})^{-k}}{C_{011}(\frac{r}{b})^{-k}}hP-\frac{\rho\omega^2r^2h}{nC_{011}(\frac{r}{b})^{-k}\kappa^n}+\frac{h}{nC_{011}(\frac{r}{b})^{-k}\kappa^n}$$
$$[\{(k+t-1)C_{011}+C_{021}\}(\frac{r}{b})^{-k}\{1-\kappa^n(P+1)^n\}+\{(k+t-1)C_{012}+C_{022}\}(\frac{r}{b})^{-k}\{1-\kappa^n\}+\{(k+t-1)C_{013}+C_{023}\}(\frac{r}{b})^{-k} \tag{13}$$
$$\{1-(1-d)^n\}]+P(P+1)^n+\frac{C_{012}(\frac{r}{b})^{-k}}{C_{011}(\frac{r}{b})^{-k}}P-\frac{k}{n}\{(P+1)^n+\frac{C_{012}(\frac{r}{b})^{-k}}{C_{011}(\frac{r}{b})^{-k}}+\frac{C_{013}(\frac{r}{b})^{-k}}{C_{011}(\frac{r}{b})^{-k}\kappa^n}(1-d^n)\}-\frac{\rho\omega^2r^2}{C_{011}(\frac{r}{b})^{-k}\kappa^n}+\frac{\rho\omega^2r^2q}{2C_{011}(\frac{r}{b})^{-k}\kappa^n}].$$

Taking asymptotic value of κ as $P\to\pm\infty$ in Eq. (13) as,

$$\frac{d\log TR}{dr}=\frac{k}{r}+\frac{C_{021}(\frac{r}{b})^{-k}-\{(1-t)C_{011}(\frac{r}{b})^{-k}\}}{rC_{011}(\frac{r}{b})^{-k}}. \tag{14}$$

Integrating Eq. (14) we get

$$TR=A_0 r^{\left(k+t-1+\frac{C_{021}(\frac{r}{b})^{-k}}{C_{011}(\frac{r}{b})^{-k}}\right)}, \tag{15}$$

where A_0 is the constant of integration.

Using Eq. (10) in Eq. (15), we get

$$\tau_{rr}=B_0[1-A_0 r^{\left(k+t-1+\frac{C_{021}(\frac{r}{b})^{-k}}{C_{011}(\frac{r}{b})^{-k}}\right)}]-\frac{\rho\omega^2r^2}{2},\quad \text{where } B_0=\frac{(C_{011}+C_{012}+C_{013})(\frac{r}{b})^{-k}}{n}. \tag{16}$$

Substituting Eq. (16) in Eq. (6), we have

$$\tau_{\theta\theta}=B_0[1-k-t-\frac{C_{021}(\frac{r}{b})^{-k}}{C_{011}(\frac{r}{b})^{-k}}A_0 r^{\left(k+t-1+\frac{C_{021}(\frac{r}{b})^{-k}}{C_{011}(\frac{r}{b})^{-k}}\right)}]+(t+q-1)\frac{\rho\omega^2r^2}{2}. \tag{17}$$

Using Eq. (2) and third equation of Eq. (5), one get

$$\tau_{zz}=\frac{C_{032}(\frac{r}{b})^{-k}}{(C_{012}+C_{022})(\frac{r}{b})^{-k}}[\tau_{rr}+\tau_{\theta\theta}]+\{C_{031}(\frac{r}{b})^{-k}-\frac{C_{032}(\frac{r}{b})^{-k}(C_{011}(\frac{r}{b})^{-k}+C_{021}(\frac{r}{b})^{-k})}{(C_{012}+C_{022})(\frac{r}{b})^{-k}}\}e_{rr}$$
$$+\{C_{033}-\frac{C_{032}(\frac{r}{b})^{-k}(C_{013}(\frac{r}{b})^{-k}+C_{023}(\frac{r}{b})^{-k})}{(C_{012}+C_{022})(\frac{r}{b})^{-k}}\}e_{zz}. \tag{18}$$

The values of constants A_0 and B_0 are obtained by substituting boundary conditions from Eq. (8) in Eq. (16) as,

$$A_0=\frac{\dfrac{\rho\omega^2(b^2-a^2)}{2}+p_1-p_2}{(\dfrac{\rho\omega^2b^2-p_2}{2})a^\alpha-(\dfrac{\rho\omega^2a^2-p_1}{2})b^\alpha},\qquad B_0=\frac{\dfrac{\rho\omega^2a^2}{2}+p_1-p_2}{1-\{\dfrac{\dfrac{\rho\omega^2(b^2-a^2)}{2}+p_1-p_2}{(\dfrac{\rho\omega^2b^2-p_2}{2})a^\alpha-(\dfrac{\rho\omega^2a^2-p_1}{2})b^{\alpha)}}\}a^\alpha},\tag{19}$$

where $\alpha=k+t-1+\dfrac{C_{021}}{C_{011}}$.

Tresca specifies that yielding in any material occurs i.e. material will flow plastically when maximum shear stress is equals to yield stress of the material. This maximum shear stress is equals to half the difference of maximum principle stress and minimum principle stress. In the classical theory, assumptions are used by the authors for this yield criterion to join the two spectrums i.e. elastic region and plastic region while in the case of transition theory this yield criterion has been calculated from the constitutive equations in transition state. Thus, from Eqs. (16) and (17),

$$|\tau_{rr}-\tau_{\theta\theta}|=\left|B_0[k+t+(\frac{C_{021}-C_{011}}{C_{011}})A_0r^\alpha]-(p+q)\frac{\rho r^2\omega^2}{2}\right|.\tag{20}$$

It can be seen from Eq. (20) that $|\tau_{rr}-\tau_{\theta\theta}|$ is maximum at $r=a$ which means yielding of the cylinder will takes place at the internal surface. Thus, Eq. (20) can be rewritten as:

$$|\tau_{rr}-\tau_{\theta\theta}|_{r=a}=|A_1\,\omega^2+A_2\,p_1-A_3\,p_2|\equiv Y\,,\tag{21}$$

where $A_1=\dfrac{\rho}{2A}[\alpha b^2-(t+q+(k-q)(\dfrac{b}{a})^\alpha+\dfrac{C_{021}-C_{011}}{C_{011}})a^2]$, $A_2=\dfrac{[(k+t)(\dfrac{b}{a})^\alpha+\dfrac{C_{021}-C_{011}}{C_{011}})]}{A}$ and $A_3=\dfrac{\alpha}{A}, A=1-\left(\dfrac{b}{a}\right)^\alpha$.

For the material to become fully plastic, the change in volume must be zero under the set of applied forces i.e. volumetric strain = 0. For full plasticity [10], $C_{11}=C_{13}=C_{12}, C_{21}=C_{23}=C_{22}, C_{31}=C_{32}=C_{33}$, Eq. (20) becomes

$$|\tau_{rr}-\tau_{\theta\theta}|_{r=b}=|B_1\omega^2+B_2p_1-B_3p_2|\equiv Y^*\;,\tag{22}$$

where $B_1=\dfrac{\rho}{2B}[(k+t)(\dfrac{a}{b})^\varsigma-(k+t)\dfrac{a^2}{b^2}+(\dfrac{C_{022}-C_{011}}{C_{011}})(1-\dfrac{a^2}{b^2})-(t+q)B]$, $B_2=\dfrac{\varsigma}{B}$ and $B_3=\dfrac{[(k+t)(\dfrac{a}{b})^\varsigma+\dfrac{C_{022}-C_{011}}{C_{011}})]}{B}$,

$\xi=k+t-1+\dfrac{C_{022}}{C_{011}}, B=1-(\dfrac{a}{b})^\alpha$.

Now we introduce the following non-dimensional component as:

$$R=(r/b),\;R_0=(a/b),\sigma_{rr}=[\tau_{rr}/Y],\sigma_{\theta\theta}=[\tau_{\theta\theta}/Y].$$

Angular speed required for initial yielding can be rewritten from Eq. (21) in non-dimensional form as:

$$\left|\frac{\rho\omega^2b^2}{Y}\right|=\Omega_i^{\,2}=\frac{1}{|A_1|}|1-A_2P_1+A_3P_2|,\text{ where } P_1=\frac{p_1}{Y}\text{ and }P_2=\frac{p_2}{Y}.\tag{23}$$

Also, angular speed required for fully plasticity can be rewritten from Eq. (22) in non-dimensional form as:

$$\left|\frac{\rho\omega^2 b^2}{Y^*}\right| = \Omega_p^2 = \frac{1}{|B_1|}\left|1 - B_2 P_1 + B_3 P_2\right|, \text{where } P_1 = \frac{p_1}{Y^*} \text{ and } P_2 = \frac{p_2}{Y^*}. \tag{24}$$

Transitional stresses are given as:

$$\sigma_{rr} = \left[\frac{\tau_{rr}}{Y}\right] = \left\{\frac{(\Omega_i^2 - P_2)R_0^{\alpha} - (\Omega_i^2 R_0^2 - P_1) - (\Omega_i^2 - \Omega_i^2 R_0^2)R^{\alpha} - (P_1 - P_2)R^{\alpha}}{R_0^{\alpha} - 1}\right\} - \Omega_i^2 R^2, \tag{25}$$

$$\sigma_{\theta\theta} = \left[\frac{\tau_{\theta\theta}}{Y}\right] = \left\{\frac{(1-k-t)(\Omega_i^2 - P_2)R_0^{\alpha} - (\Omega_i^2 R_0^2 - P_1) - \dfrac{C_{021}}{C_{011}}(\Omega_i^2 - \Omega_i^2 R_0^2 + P_1 - P_2)R^{\alpha}}{R_0^{\alpha} - 1}\right\} + (t+q-1)\Omega_i^2 R^2. \tag{26}$$

Stresses for full plasticity [10] $C_{11} = C_{13} = C_{12}$, $C_{21} = C_{23} = C_{22}$, $C_{31} = C_{32} = C_{33}$ are given as:

$$\sigma_{rr}^* = \left[\frac{\tau_{rr}}{Y^*}\right] = \left\{\frac{(\Omega_p^2 - P_2)R_0^{\varsigma} - (\Omega_p^2 R_0^2 - P_1) - (\Omega_p^2 - \Omega_p^2 R_0^2)R^{\varsigma} - (P_1 - P_2)R^{\varsigma}}{R_0^{\varsigma} - 1}\right\} - \Omega_p^2 R^2, \tag{27}$$

$$\sigma_{\theta\theta}^* = \left[\frac{\tau_{\theta\theta}}{Y^*}\right] = \left\{\frac{(1-k-t)(\Omega_p^2 - P_2)R_0^{\varsigma} - (\Omega_p^2 R_0^2 - P_1) - \dfrac{C_{022}}{C_{011}}(\Omega_p^2 - \Omega_p^2 R_0^2 + P_1 - P_2)R^{\varsigma}}{R_0^{\varsigma} - 1}\right\} + (t+q-1)\Omega_p^2 R^2. \tag{28}$$

The Eqs. (27) and (28) are fully plastic stresses for orthotropic cylinder made up of functionally graded material under internal and external pressure.

If we substitute $k = 0$, $t = 0, q = 0, P_1 = P_2 = 0$ in Eq. (4), Eq. (6), we have

$$C_{ij} = C_{0ij},\ h = h_0,\ \rho = \rho_0. \tag{29}$$

Using Eq. (29) in Eqs. (27-28), the radial, circumferential stresses of orthotropic cylinder becomes

$$\sigma_{rr}^* = \left[\frac{\tau_{rr}}{Y^*}\right] = \left\{\frac{\Omega_p^2 R_0^{\zeta} - \Omega_p^2 R_0^2 - (\Omega_p^2 - \Omega_p^2 R_0^2)R^{\zeta}}{R_0^{\zeta} - 1}\right\} - \Omega_p^2 R^2, \tag{30}$$

$$\sigma_{\theta\theta}^* = \left[\frac{\tau_{\theta\theta}}{Y^*}\right] = \left\{\frac{(1-k-t)\Omega_p^2 R_0^{\zeta} - \Omega_p^2 R_0^2 - \dfrac{C_{022}}{C_{011}}(\Omega_p^2 - \Omega_p^2 R_0^2)R^{\zeta}}{R_0^{\zeta} - 1}\right\} + (t+q-1)\Omega_p^2 R^2, \text{where } \xi = \frac{(C_{22} - C_{11})}{C_{11}} \tag{31}$$

The Eqs. (30) and (31) are same as obtained by Gupta [10] for orthotropic cylinder made up of homogeneous material.

6 RESULTS AND NUMERICAL DISCUSSION

The material properties of the cylinder made up of functionally graded orthotropic material (Barite and Topaz) and isotropic material (Mild Steel) are defined as:

Table 1
Elastic constants C_{ij} used (in units of 10^{11} N/m^2).

Materials	C_{11}	C_{12}	C_{13}	C_{21}
Steel (Isotropic Material)	2.908	1.27	1.27	2.908
Barite (Orthotropic Material)	0.907	0.273	0.275	0.273
Topaz (Orthotropic Material)	2.813	1.258	0.846	1.258

The inner and outer radii of the cylinder are taken as a = 1 and b = 2 respectively. To calculate the transitional and fully plastic stresses based on the above analysis Eq. (23) to Eq. (28) have been evaluated by the use of Mathematica. Curves have been made for angular speed required for initial yielding and fully plastic state with respect to radii ratio R_0 as shown in Figs. 1-4 for k= -5, -4, -3, -2 respectively under various internal and external pressure.

It has been observed from Fig. 1 and Tables 2-4, that angular speed required for initial yielding in a rotating cylinder under internal and external pressure is maximum at the external surface. It has also been observed that high angular speed is required for initial yielding for the rotating cylinder made up of less non-homogeneous material as compared to rotating cylinder made up of highly non-homogeneous material. It has been noticed from Table 2, Table 3 and Table 4 that angular speed required for initial yielding is maximum for orthotropic material i.e. topaz as compared to orthotropic material i.e. barite and isotropic material i.e. mild steel. It has also been observed that with the decrease in non-homogeneity (k = -2 to k = -5) angular speed required for initial yielding increases significantly. It has been noticed from Fig. 2 that with the increase in internal and external pressure angular speed required for initial yielding increases significantly for rotating cylinder made up of orthotropic and isotropic materials.

It has been observed from Fig. 3, Table 2, Table 3, and Table 4 that angular speed required for fully plastic state is maximum at the internal surface for rotating cylinder made up of orthotropic and isotropic materials. It has also been observed that angular speed required for full plasticity is less for highly non-homogeneous rotating cylinder. It has also been observed that angular speed required for fully plasticity decreases with the increase in non-homogeneity of rotating cylinder under internal and external pressure.

It has been noticed from Tables 2-4, that percentage increase in angular velocity required for initial yielding to become fully plastic is high for isotropic material as compared to orthotropic materials at the internal surface. Also this percentage increase in angular velocity is maximum for less non-homogeneous rotating cylinder as compared to highly non-homogeneous rotating cylinder. Out of two orthotropic materials i.e. barite and topaz, angular speed required for initial yielding to become fully plastic is high for barite as compared to topaz. With the increase in pressure, this percentage increases significantly as can be seen from Tables 5-7. It has also been observed that angular speed required for full plasticity is high for orthotropic material barite as compared to orthotropic material topaz and isotropic material mild steel. It has been noticed from Fig. 2 that with the increase in internal and external pressure angular speed required for initial yielding increases significantly for rotating cylinder made up of orthotropic and isotropic materials. It can be seen from Fig. 4 that with the increase in pressure, angular speed required for full plasticity increases significantly for both orthotropic and isotropic materials.

Table 2
Percentage in angular speed required for initial yielding to become fully plastic state for the orthotropic cylinder made up of barite material under internal pressure = 2 and external pressure = 0.5.

	k	Ω^2 / R_0	0.2	0.4	0.6	0.2	0.4	0.6
Internal Pressure=2 External Pressure=0.5	-5	Initial Yielding	0.0196756	0.0782957	0.162032	96.064	84.132	61.844
		Full Plasticity	0.499902	0.493412	0.424652			
	-4	Initial Yielding	0.0196068	0.0773809	0.149209	96.075	84.004	60.221
		Full Plasticity	0.499517	0.483754	0.375098			
	-3	Initial Yielding	0.0194884	0.0752184	0.123576	96.084	83.655	57.863
		Full Plasticity	0.497633	0.460204	0.293273			
	-2	Initial Yielding	0.0192104	0.0694246	0.065533	96.068	82.808	59.029
		Full Plasticity	0.488589	0.403819	0.15995			

Table 3
Percentage in angular speed required for initial yielding to become fully plastic state for the orthotropic cylinder made up of topaz material under internal pressure = 2 and external pressure = 0.5.

	k	Ω^2 / R_0	0.2	0.4	0.6	0.2	0.4	0.6
Internal Pressure=2 External Pressure=0.5	-5	Initial Yielding	0.0211374	0.0841131	0.174897	95.771	82.855	57.466
		Full Plasticity	0.499804	0.490602	0.411193			
	-4	Initial Yielding	0.0213603	0.0843304	0.164596	95.72	82.331	53.6349
		Full Plasticity	0.499054	0.477277	0.355			
	-3	Initial Yielding	0.0216771	0.0838446	0.142756	95.625	81.2	46.1798
		Full Plasticity	0.495519	0.445974	0.265246			
	-2	Initial Yielding	0.0221154	0.0808243	0.090883	95.389	78.499	29.0805
		Full Plasticity	0.479644	0.375913	0.12815			

Table 4
Percentage in angular speed required for initial yielding to become fully plastic state for the cylinder made up of isotropic material under internal pressure = 2 and external pressure = 0.5.

	k	Ω^2 / R_0	0.2	0.4	0.6	0.2	0.4	0.6
Internal Pressure=2 External Pressure=0.5	-5	Initial Yielding	0.0210355	0.0837079	0.173999	95.7919	83.0143	58.7234
		Full Plasticity	0.499884	0.492814	0.421544			
	-4	Initial Yielding	0.0212381	0.0838462	0.163521	95.7475	82.6174	55.8530
		Full Plasticity	0.49943	0.482358	0.370401			
	-3	Initial Yielding	0.0215246	0.0832431	0.141413	95.6711	81.7877	50.6532
		Full Plasticity	0.497232	0.457072	0.28657			
	-2	Initial Yielding	0.0219131	0.0800279	0.0891004	95.4987	79.8623	41.3056
		Full Plasticity	0.486822	0.397403	0.151804			

Table 5
Percentage in angular speed required for initial yielding to become fully plastic state for the orthotropic cylinder made up of barite material under internal pressure = 3 and external pressure = 1.

	k	Ω^2 / R_0	0.2	0.4	0.6	0.2	0.4	0.6
Internal Pressure=3 External Pressure=1	-5	Initial Yielding	0.0373455	0.148935	0.319417	96.265	84.955	64.003
		Full Plasticity	0.999849	0.989961	0.887354			
	-4	Initial Yielding	0.0368102	0.146073	0.30047	96.316	85.02	62.999
		Full Plasticity	0.999251	0.975088	0.812056			
	-3	Initial Yielding	0.0359897	0.140838	0.263744	96.388	84.991	61.542
		Full Plasticity	0.996298	0.938373	0.685791			
	-2	Initial Yielding	0.0345259	0.129363	0.181622	96.484	84.754	61.68
		Full Plasticity	0.98185	0.84849	0.473966			

Table 6
Percentage in angular speed required for initial yielding to become fully plastic state for the orthotropic cylinder made up of topaz material under internal pressure = 3 and external pressure = 1.

	k	Ω^2 / R_0	0.2	0.4	0.6	0.2	0.4	0.6
Internal Pressure=3 External Pressure=1	-5	Initial Yielding	0.0392945	0.156705	0.336841	96.069	84.101	61.1422
		Full Plasticity	0.999698	0.985639	0.866855			
	-4	Initial Yielding	0.0391484	0.155372	0.32144	96.079	83.899	58.836
		Full Plasticity	0.998529	0.965009	0.780877			
	-3	Initial Yielding	0.0389094	0.152419	0.290089	96.081	83.356	54.7177
		Full Plasticity	0.992944	0.915752	0.640624			
	-2	Initial Yielding	0.0384054	0.144748	0.216741	96.029	81.947	47.9497
		Full Plasticity	0.967176	0.801784	0.416407			

Table 7
Percentage in angular speed required for initial yielding to become fully plastic state for the cylinder made up of isotropic material under internal pressure = 3 and external pressure = 1.

	k	Ω^2 / R_0	0.2	0.4	0.6	0.2	0.4	0.6
Internal Pressure=3 External Pressure=1	-5	Initial Yielding	0.0391587	0.156164	0.335625	96.0834	84.2106	61.9746
		Full Plasticity	0.999821	0.989043	0.882633			
	-4	Initial Yielding	0.0389855	0.154724	0.319974	96.0980	84.0970	60.2418
		Full Plasticity	0.999117	0.972922	0.804801			
	-3	Initial Yielding	0.038706	0.151612	0.288241	96.1125	83.7574	57.3038
		Full Plasticity	0.995664	0.933423	0.675097			
	-2	Initial Yielding	0.0381351	0.143672	0.214268	96.1046	82.8536	53.3947
		Full Plasticity	0.97898	0.837914	0.45975			

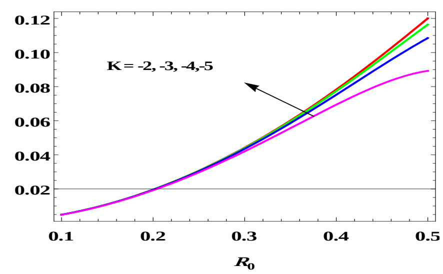

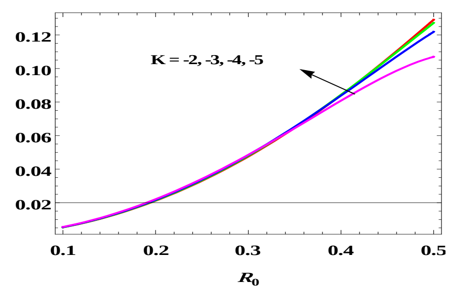

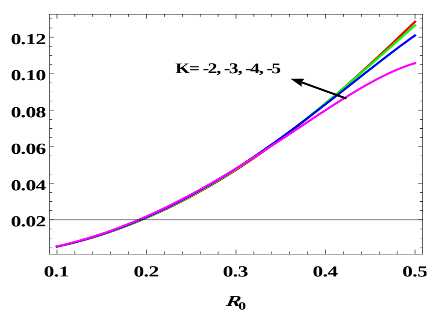

Fig.1
Angular speed required for initial yielding for Barite, Topaz and Mild Steel respectively with ($P_1 = 2$ and $P_2 = 0.5$) .

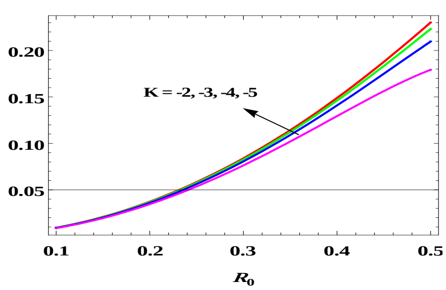

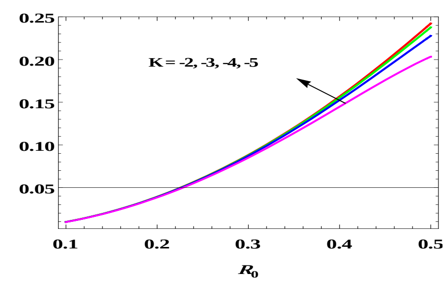

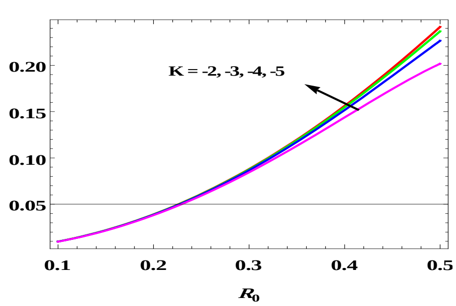

Fig.2
Angular speed required for initial yielding for Barite, Topaz and Mild Steel respectively with ($P_1 = 3$ and $P_2 = 1$) .

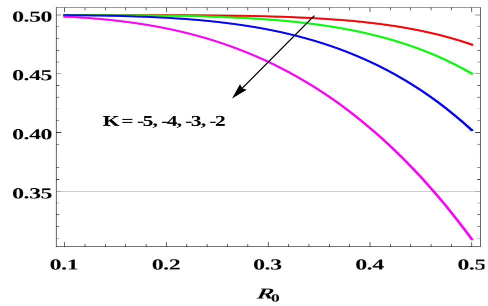

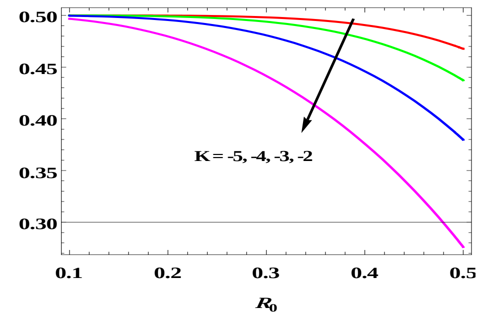

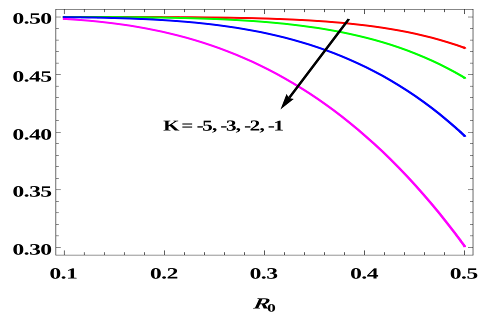

Fig.3
Angular speed required for fully plastic state for Barite, Topaz and Mild Steel respectively with $(P_1 = 2 \text{ and } P_2 = 0.5)$.

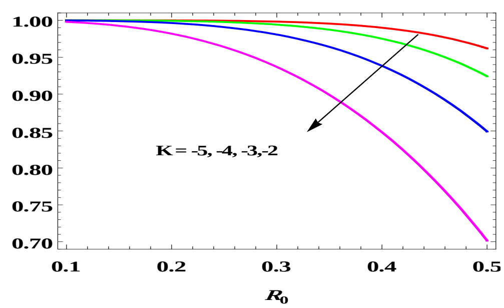

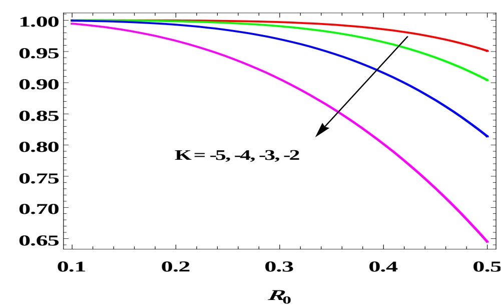

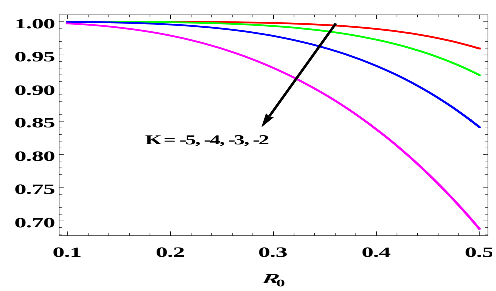

Fig.4
Angular speed required for fully plastic state for Barite, Topaz and Mild Steel respectively with $(P_1 = 3 \text{ and } P_2 = 1)$.

It has been observed from Table 8, that circumferential transitional stresses are maximum at the internal surface for rotating cylinder under internal and external pressure with angular speed $\Omega^2 = 5$. From Fig. 5, it has also been noticed that circumferential transitional stresses are less for highly non-homogeneous rotating cylinder and these stresses increases with the decrease in non-homogeneity. Also, these circumferential transitional stresses are high for barite as compared to topaz and mild steel. From Fig. 6, it can be seen that with the increase in pressure, circumferential stresses decrease significantly which further decrease with the increase in pressure. It has been observed from Table 9 that fully plastic circumferential stresses are maximum at the internal surface for isotropic rotating cylinder i.e. mild steel while these stresses are maximum at the centre of the cylinder for orthotropic rotating cylinder made up of barite and topaz. Also, from Fig. 7, it can be seen that these circumferential stresses are high for less non-homogeneous rotating cylinder as compared to highly non-homogeneous rotating cylinder. Also circumferential stresses are high for cylinder made up of isotropic material as compared to orthotropic material. It has also been noticed from Table 9, Fig. 8 that with the increase in pressure these circumferential stresses decrease significantly.

Table 8
Transitional circumferential stresses under internal and external pressure with angular speed ($\Omega^2 = 5$) for barite, topaz and mild steel materials respectively.

		Barite			Topaz			Mild Steel		
	k/R	0.5	0.75	1	0.5	0.75	1	0.5	0.75	1
Internal Pressure=2 External Pressure=0.5	-5	28.9679	28.8954	26.7981	28.2242	28.8682	26.8219	22.634	28.476	26.759
	-3	20.5375	20.3739	18.3677	19.8325	20.335	18.4302	14.0501	19.4203	18.1751
Internal Pressure=3 External Pressure=1	-5	25.2916	25.3611	23.2723	24.4713	25.3254	23.2926	18.3495	24.8967	23.2245
	-3	17.8209	17.7906	15.8016	17.0322	17.7314	15.8535	10.7013	16.7318	15.5763
Internal Pressure=4 External Pressure=1.5	-5	21.6153	21.8267	19.7465	20.7184	21.7827	19.7633	14.065	21.3173	19.69
	-3	15.1043	15.2072	13.2355	14.2319	15.1278	13.2768	7.35249	14.0432	12.9775

Table 9
Fully plastic circumferential stresses under internal and external pressure with angular speed ($\Omega^2 = 5$) for barite, topaz and mild steel materials respectively.

		Barite			Topaz			Mild Steel		
	k/R	0.5	0.75	1	0.5	0.75	1	0.5	0.75	1
Internal Pressure=2 External Pressure=0.5	-5	26.0228	28.7654	26.9035	23.583	28.6041	27.0159	30.7619	22.8	17
	-3	17.7572	20.1831	18.6379	15.4769	19.9358	18.9099	29.1994	21.2375	15.4375
Internal Pressure=3 External Pressure=1	-5	22.0388	25.1914	23.3605	19.3334	12.1012	5.68568	27.2222	20.2	15.3333
	-3	14.6976	17.5033	16.0193	24.9815	17.1336	9.7448	25.6597	18.6375	13.7708
Internal Pressure=4 External Pressure=1.5	-5	18.0549	21.6175	19.8175	15.0838	21.3589	19.8849	23.6825	17.6	13.6667
	-3	11.638	14.8235	13.4006	8.72546	14.3313	13.5266	22.12	16.0375	12.1042

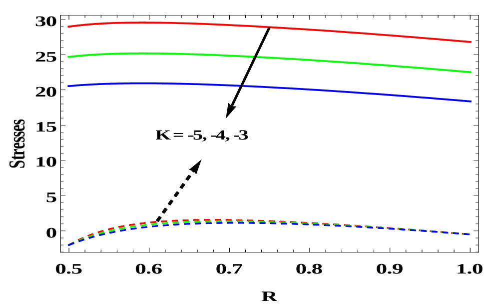

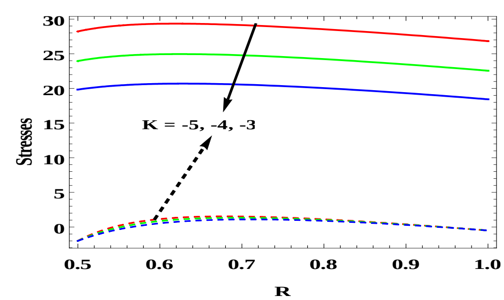

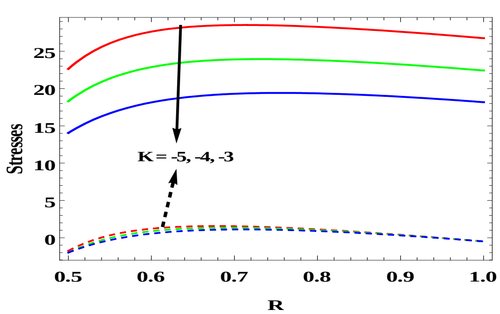

Fig.5
Transitional circumferential stresses for Barite, Topaz and Mild Steel respectively with ($P_1 = 2$ and $P_2 = 0.5$) .

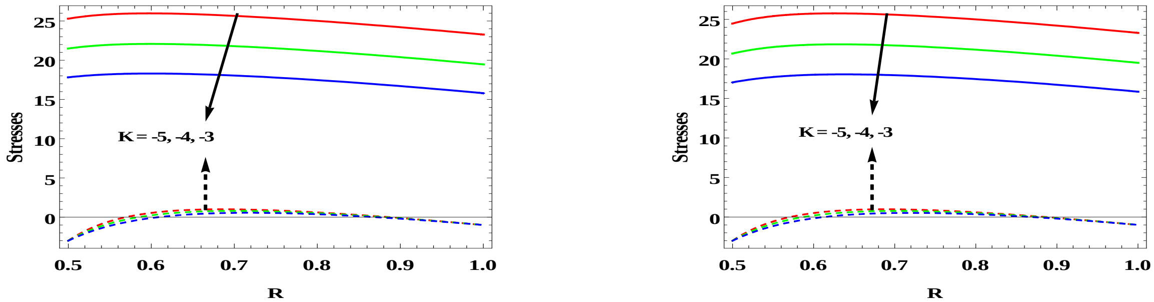

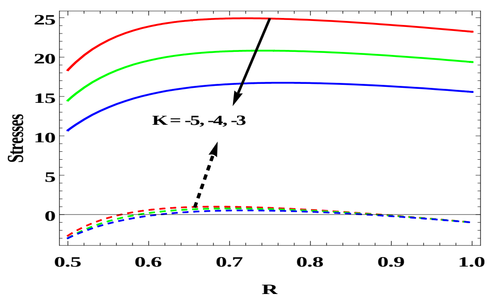

Fig.6
Transitional circumferential stresses for Barite, Topaz and Mild Steel respectively with ($P_1 = 3$ and $P_2 = 1$) .

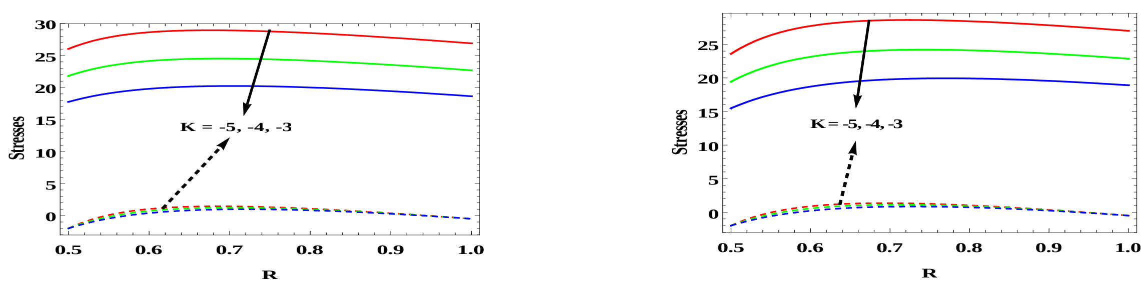

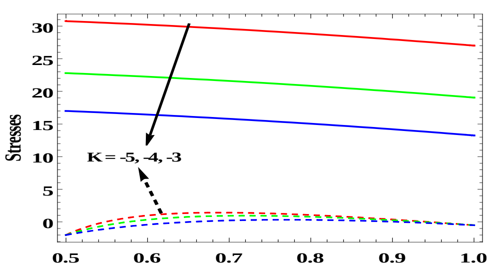

Fig.7
Fully plastic circumferential stresses for Barite, Topaz and Mild Steel respectively with ($P_1 = 2$ and $P_2 = 0.5$) .

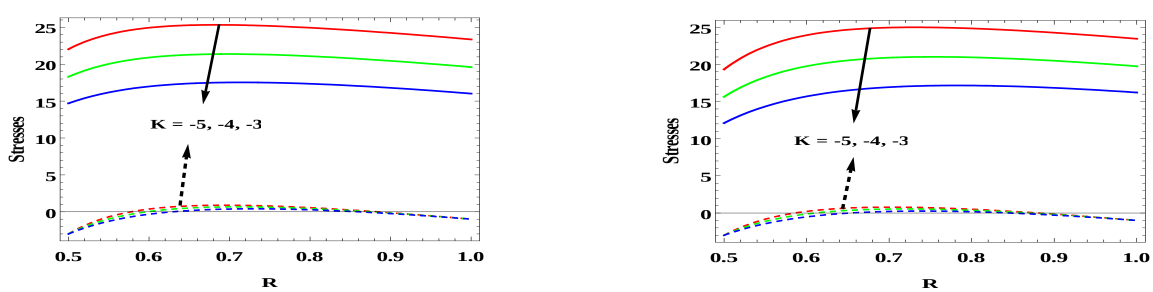

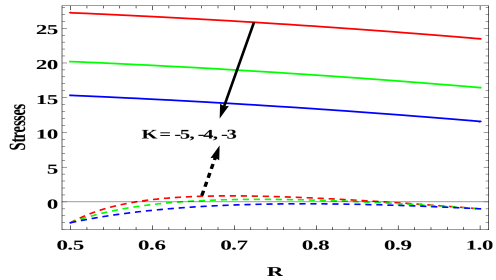

Fig.8
Fully plastic circumferential stresses for Barite, Topaz and Mild Steel respectively with $(P_1 = 3 \text{ and } P_2 = 1)$.

7 CONCLUSIONS

On the basis of above discussion, it has been concluded that circular cylinder made up of highly functionally graded orthotropic material (Topaz) under internal and external pressure is better choice for designing as compared to cylinder made up of functionally graded orthotropic material (Barite) and isotropic material (Mild Steel). It is because of the reason that circumferential stresses are less for Topaz as compared to Steel and Barite. Also, the cylinder whose thickness increases radially and density decreases radially is on the safer side of design. This leads to the idea of stress savings that minimizes the possibility of fracture of cylinder due to internal and external pressure.

REFERENCES

[1] Bower A.F., 2009, *Applied Mechanics of Solids*, Taylor and Francis.
[2] Hearn E.J., 1997, *Mechanics of Materials*, Butterworth-Heinemann.
[3] Kim J.H., Paulino G.H., 2004, T-stress in orthotropic functionally graded materials: Lekhnitskii and Stroh formalisms, *International Journal of Fracture* **126**: 345-384.
[4] Zenkour A.M., 2006, Rotating variable-thickness orthotropic cylinder containing a solid core of uniform-thickness, *Archive Applied Mechanics* **76**: 89-102.
[5] Dag S., 2006, Thermal fracture analysis of orthotropic functionally graded materials using an equivalent domain integral approach, *Engineering Fracture Mechanics* **73**: 2802-2828.
[6] Paschero M., Hyer M.W., 2009, Axial buckling of an orthotropic circular cylinder: Application to orthogrid conceptual, *International Journal of Solids and Structures* 46: 2151-2171.
[7] Wang H.M., 2010, Effect of material in-homogeneity on the rotating functionally of a graded orthotropic hollow cylinder, *Journal of Mechanical Science and Technology* **24**(9): 1839-1844.
[8] Nie G.J., Batra R.C., 2010, Static deformations of functionally graded polar-orthotropic cylinders with elliptical inner and circular outer surfaces, *Composites Science and Technology* **70**: 450-457.
[9] Sharma S., Yadav S., 2013, Thermo elastic-plastic analysis of rotating functionally graded stainless steel composite cylinder under internal and external pressure using finite difference method, *Advances in Materials Science and Engineering* **2013**: 1-10.
[10] Gupta S.K., Bhardwaj P.C., 1986, Elastic plastic and creep transition in orthotropic rotating cylinder, *Processing Indian National Science Academy* **52**(6): 1357-1369.
[11] Borah B.N., 2005, Thermo elastic plastic transition, *Contemporary Mathematics* **379**: 93-111.
[12] Aggarwal A.K., Sharma R., Sharma S., 2013, Safety analysis using Lebesgue strain measure of thick-walled cylinder for functionally graded material under internal and external pressure, *The Scientific World Journal* **2013**: 1-10.
[13] Sharma S., Sahai I., Kumar R. , 2014, Thermo elastic-plastic transition of transversely isotropic thick-walled circular cylinder under internal and external pressure, *Multidiscipline Modeling in Materials and Structures* **10**: 211-227.
[14] Sharma S., Yadav S., Sharma R., 2017, Thermal creep analysis of functionally graded thick-walled cylinder subjected to torsion and internal and external pressure, *Journal of Solid Mechanics* **9**(2): 302-318.